Earth Materials and Processes

The Earth Materials and Processes area comprises groups in Experimental Petrology, Rock Physics, Thermochronology, and Structure & Tectonics. Our research centres around laboratory based measurements under controlled conditions, simulating those occurring in nature, but these activities are complimented by a rich array of analytical equipment and are supported by extensive field-based observations, often in collaboration with scientists from other institutions, nationally and internationally. Through such investigations we are developing understanding of the structure and chemical composition of planetary interiors, and the processes by which they evolve. Our interests start at the very beginning of solar system history with how the Earth and other rocky planets accrete, but also covers the ongoing processes of mantle convection, volcanism, metamorphism, global tectonics and the formation of ore deposits.

Areas of current research activity include:

- The making of terrestrial planets. Chemical constraints on the accretion of the Earth and similar planets from the solar nebula, and the processes of core formation; mineralogical and chemical properties of the deep mantle and their influence on global tectonics.

- The nature of the Earth's upper mantle. Experimental studies and thermodynamic modelling of the phase equilibria relevant to upper mantle melting and ultra-high-pressure metamorphism associated with crustal thickening and subduction; experimental and microstructural studies of phenomena associated with lattice defects and grain boundaries including incorporation of water into nominally anhydrous minerals and microscopic mechanisms of seismic wave attenuation; experimental studies and modelling of grain-scale melt distribution and its implications for melt transport, rheology and seismic properties.

- Coupling between fluid flow and fault mechanics in the continental crust Experimental studies of the role of fault healing and sealing processes in controlling the time dependence of fault strength and permeability at high temperatures and pressures; complementary field-based and modelling studies exploring fluid-driven growth of shear networks with applications to understanding the development of lode gold systems, especially in the Western Australian goldfields.

- Oxidation state and coordination of metal ions at high temperatures. Studies of crystals, melts and hydrothermal solutions by X-ray absorption spectroscopy, using synchrotron radiation. Studies of silicate glasses and melts to very high temperatures under controlled redox conditions. Analysis of hydrothermal solutions trapped in synthetic fluid inclusions is providing important basic information on metal complexes at high temperatures.

Experimental Petrology Introduction

The Experimental Petrology Group uses a laboratory-based experimental approach combined with field observations to study the Earth, its origin, evolution and mineral wealth. The group operates a wide range of experimental apparatuses for generating the high temperatures and pressures that are needed to reproduce the natural conditions within the Earth. The equipment includes: high temperature furnaces capable of reaching 1800°C, several of which are equipped for precise control of oxygen and sulfur fugacities by gas mixing; eleven solid-media piston-cylinder devices for generating pressures to 6 GPa and temperatures in excess of 2000°C, a multi-anvil apparatus, which can presently achieve pressures of 27 GPa; and a well-equipped hydrothermal laboratory.

These high-temperature, high-pressure apparatuses are complimented by an array of microbeam analytical techniques, including a Cameca SX100 electron microprobe; laser-ablation ICP-MS, which is now being used regularly to analyse trace-elements in experimental run products; a STOE STADIP powder X-ray diffractometer; and FTIR spectroscopy for the determination of H2O, CO2 and other volatile species in minerals and glasses. To complement this latter facility, the group acquired a Agilent 6850 Gas Chromatograph, which has been combined with a capsule-piercing device to enable the extraction and analysis of small quantities of C-O-H fluids from high-pressure experimental run products.

As well as the conventional 1/2 inch and 5/8 inch apparatus for use to 4 GPa, the group's piston-cylinder laboratory also runs a high-pressure device that is now operating regularly at 6.5 GPa; the laboratory also has two large-capacity piston-cylinder devices that take 30 mm and 50 to 65 mm diameter pressure assemblies respectively, enabling pressure to be controlled extremely accurately, and which are capable of synthesising relatively large volumes of high pressure phases for detailed mineralogical studies. A novel diamond composite hard material, developed in these apparatuses and now under commercial production, offers promise as an anvil material to extend the pressure range of the multi-anvil apparatus above 26 GPa, thereby allowing detailed experimental exploration of the pressure-temperature regime of the Earth's lower mantle. To further this research the multi-anvil apparatus has now been refurbished and provided with full computer control of pressure and temperature.

In recent years the group has become increasingly involved in developing methods to characterise geologic materials by X-ray absorption spectroscopy (XANES) and related techniques that use synchrotron radiation. Research in this area is presently concentrating on oxidation states in silicate melts, including in-situ measurements at temperatures to 1500°C, and speciation in ore-forming hydrothermal solutions. Members of the group continue to investigate conditions and processes in the Earth's upper mantle (Professors David Green and Hugh O'Neill, Dr Robert Rapp), and metamorphism in the continental crust (Dr Joerg Hermann), as well as the physical chemistry of ore-forming solutions (Drs John Mavrogenes, Katy Evans).

On twinning and microstructures in calcite and dolomite

Andrew G. Christy[1], Ann-Kristin Larsson[2]

[1] *Research School of Earth Sciences, Australian National University, Canberra, ACT 0200, Australia*
[2] *Research School of Chemistry, Australian National University, Canberra, ACT 0200, Australia*

Electron diffraction of the rhombohedral carbonate minerals can show additional diffraction spots which have been ascribed to various metastable Ca-Mg ordering schemes that remain unknown as macroscopic minerals. We have found that such reflexions can be produced by nanoscale twin domains which appear to be widespread in both biogenic and abiogenic carbonates. Because of the many metrical pseudosymmetries in the calcite structure, such twins can produce diffraction resembling that of commensurate modulated structures. Twin nanodomains on {104}, in particular, can produce the diffraction patterns of any of the supposed "g", "m" and "n" superstructures, provided only that the usual carbonate orientational order is lost in the twin. Thus, these superstructures may not actually exist, and controversies surrounding their occurrence may not be irrelevant. {018} twins are also common, and diffract similarly to a fivefold superstructure.

Larsson A-K, Christy AG (2008) On twinning and microstructures in calcite and dolomite. *Amer. Mineral.* **93**: 103-113.

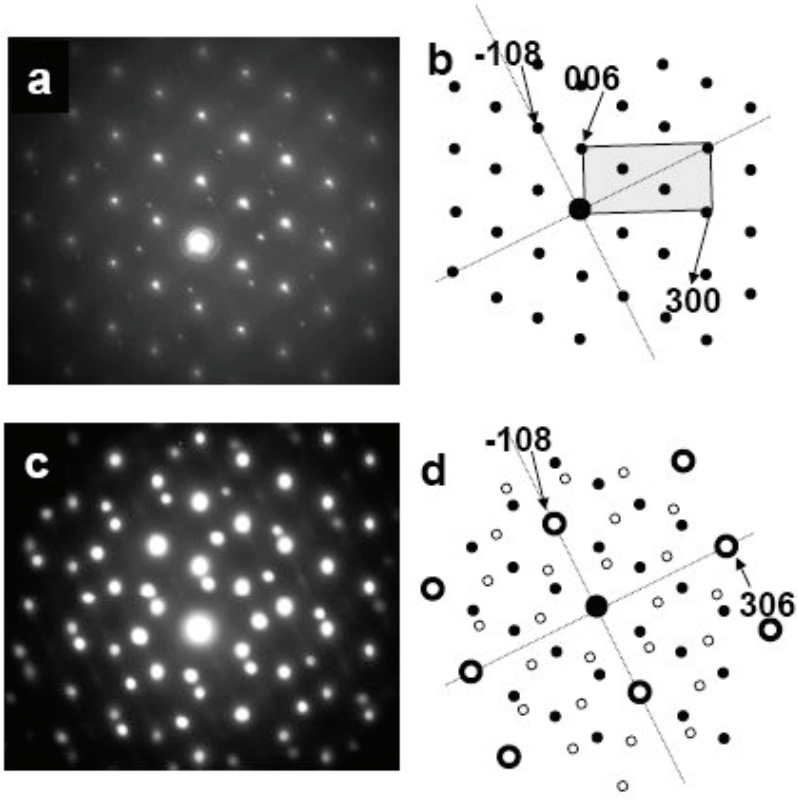

Figure 1. Electron diffraction patterns of a calcite crystal from a sea urchin shell. (a) Selected area is about 1 mm diameter, weak diffraction can be seen that is additional to that of the host crystal. (b) Indexed, consistent with viewing direction [010]. (c) Smaller selected area of 100 nm diameter, enhancing reflexions from a small {018} twin domain which gives trhe appearance of a fivefold superstructure.

Multiple element diffusivities in natural olivine xenocryst from high-Mg diorite

Jörg Hermann[1], Qian Qing[1], Hugh St.C. O'Neill[1]

[1] *Research School of Earth Sciences, The Australian National University, Canberra, ACT 0200, Australia*

Despite solid-state diffusion being central to many geological processes, little is known about the factors controlling the rates of diffusion of different species in silicate minerals. Theoretical modeling of diffusivities in silicates suffers from a general lack of empirical data against which the modeling can be tested.

Olivine xenocrysts (0.5-3 mm in diameter, up to 20% in volume) were found in the chilled margin of one of the plutons of high-Mg diorite from Handan-Xingtai, central North China block, which was formed at an intracontinental setting. These hybridized high-Mg dioritic rocks formed during cooling from ~ 1000°C. One crystal with favorable dimensions and orientation, and despite some dissolution still retaining a crystal face, indicating minimal dissolution (Fig. 1), was selected for detailed study. Concentration profiles of Mg, Fe, Mn and Ni were determined by electron microprobe. The olivine was normally zoned in Mg/Fe, with Fo# [100*Mg/(Mg + Fe^T)] decreasing from core (89.1-93.2) to rim (73.2-81.4). Element mapping with the electron microprobe showed a gradual change of Fe, Mg, and Mn contents (Fig. 2). Concentration profiles of trace elements (Li, Na, Al, P, Ca, Sc, Ti, V, Cr, Mn, Co, Ni and Y) were then determined along the same or similar profiles by laser-ablation inductively-coupled plasma mass spectrometry (LA-ICP-MS). The profiles were acquired using different spot sizes as well as continuing scans using a 7 x 70 µm slit (Fig. 2).

The obtained data (Fig. 3) allow trace diffusion coefficients to be evaluated relative to Mg-Fe interdiffusion under conditions that cannot be accessed in the laboratory. The effective diffusion coefficients of many trace elements (Li, Ca, Sc, Mn, Co, Ni and Y) fall within a factor of three of each other and of the mean Mg-Fe interdiffusion coefficient, in agreement with results from laboratory experiments at higher temperatures (Spandler et al. 2007). By contrast, the profiles for Na, Ti and V imply much faster diffusion rates, while P shows no discernible diffusion. The Al and Cr profiles, which are well correlated with each other, are highly complex and variable on a small length scale. These data show that the diffusion coefficients of cations in olivine are not simple functions of either ionic charge or ionic radius. Using published Mg-Fe interdiffusion coefficients (Dohmen and Chakraborty, 2007), the characteristic residence time of the olivine xenocryst is modeled to be about 10^2 to 10^3 years.

Dohmen R, Chakraborty S (2007) Fe-Mg diffusion in olivine _: point defect chemistry, change of diffusion mechanisms and a model for calculation of diffusion coefficients in natural olivine. *Physics and Chemistry of Minerals* **34**, 409-430, doi: 10.1007/s00269-007-0158-6

Spandler C, O'Neill, HStC. Kamenetsky V.S. (2007) Survival times of anomalous melt inclusions from element diffusion in olivine and chromite. *Nature* **447**, 303-306. doi: 10.1038/nature05759.

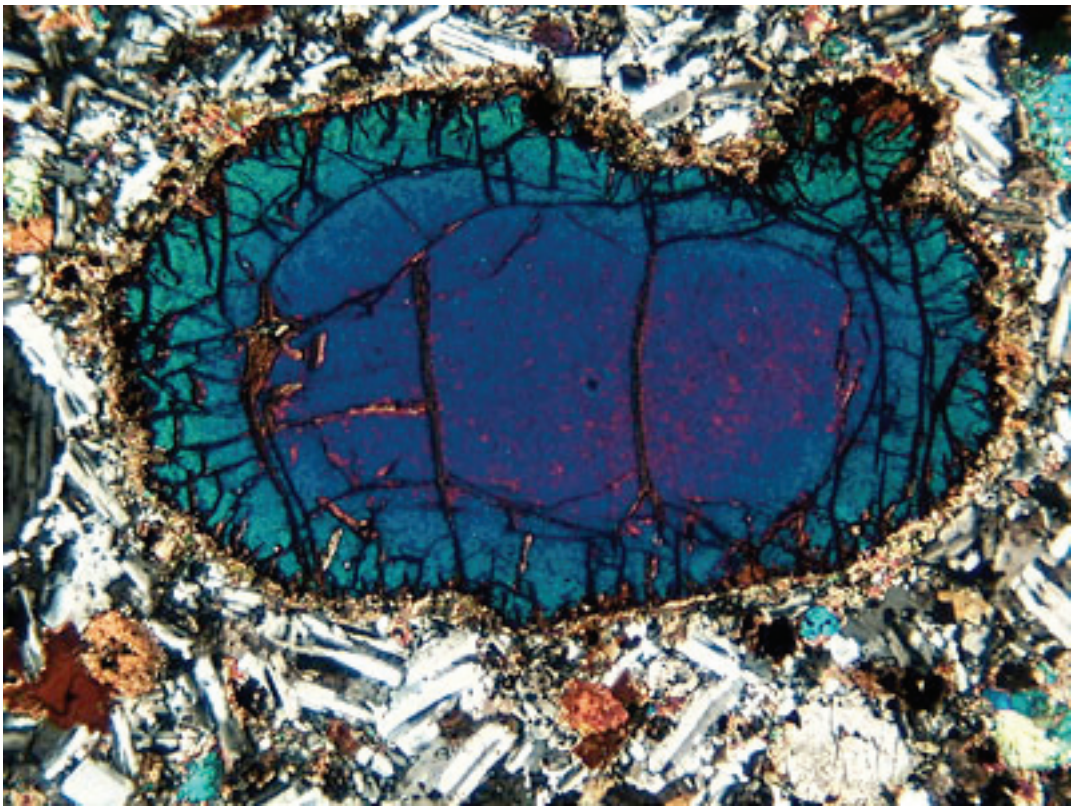

Figure 1. Microphotograph (X Nicols) of an olivine xenocrist embedded in a diorite matrix consisting of plagioclase, clinopyroxene, amphibole, biotite and quartz. The olivine grain is surrounded by a small corona of orthopyroxene. The change in interference colors from core to rim is related with an increase in fayalite component in olivine.

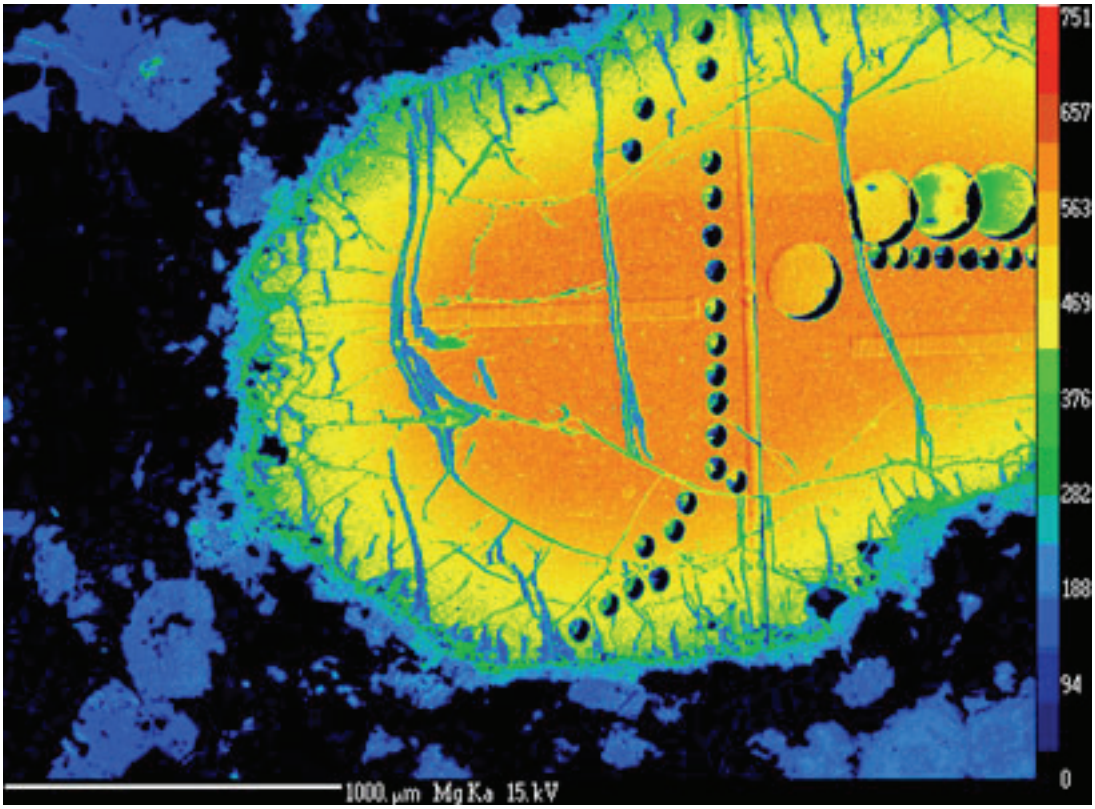

Figure 2. Mg distribution X-ray map of the investigated olivine. Mg continuously decreases from core to rim. Also shown are the different ablation pits (180 µm, 70 µm spot size) and the tracks from the LA-ICP-MS analyses.

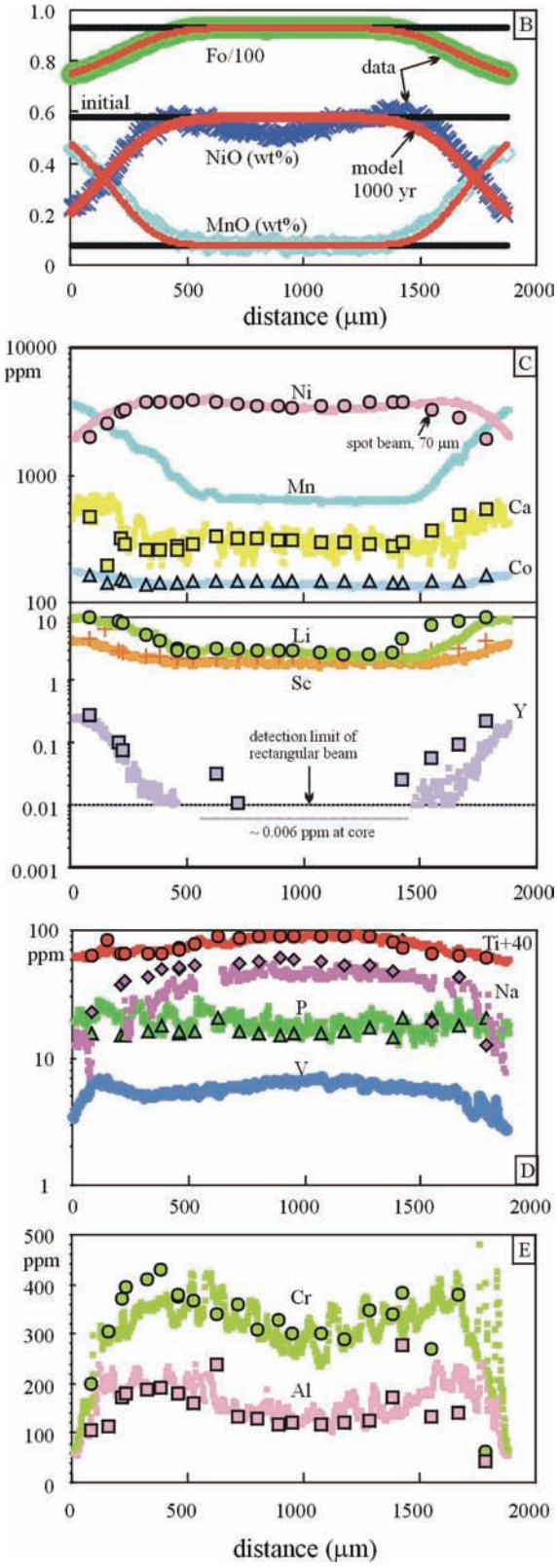

Figure 3. Profiles through the olivine grain. B) Major element data for the forsterite content and NiO and MnO in wt.% from electron microprobe analysis. The red line refers to modeled diffusion profiles indicating that the olivine had a ~1000 year residence time at 950-1000°C. C), D) and E) Trace element profiles in olivine determined with LA-ICP-MS analyses (all values in ppm). Continuous lines were measured in scan mode whereas symbols refer to single spot analyses. Note the similar diffusion behavior of ions with different charges such as Li (1+), Mn (2+) and Y (3+).

Determination of Selenium Concentrations in NIST SRM 610, 612, 614 and Reference Materials using the Electron Probe, LA-ICP-MS and SHRIMP II

Frances E Jenner[1], Peter Holden[1], John A. Mavrogenes[1],
Hugh St.C. O'Neill and Charlotte M. Allen

[1] *Research School of Earth Sciences, Australian National University, Canberra, ACT 0200, Australia*

Selenium (Se) is a trace element with distinctive geochemical properties, which have yet to be exploited in petrology because of the analytical difficulties associated with its low concentrations in geological materials. Selenium (Se) has 6 naturally occurring stable isotopes; ^{74}Se, ^{76}Se, ^{77}Se, ^{78}Se, ^{80}Se and ^{82}Se and is both volatile and strongly siderophile. Constraining the range of Se concentrations in mantle-derived rocks is important to studies of planetary differentiation, partial melting models and recycling of lithospheric components into the mantle.

The abundance of Se in the mantle is not well known, but has been estimated to be 79 ppb by assuming chondritic Se/S (Palme and O'Neill 2003). Due to the time-consuming and often complicated sample preparation techniques used by previous studies (see Johnson and Bullen 2004 for a comprehensive review) and the high levels of analytical sensitivity required, little is known about the behaviour of Se in igneous systems.

In situ analysis of geological materials such as natural volcanic glasses and minerals, using LA-ICP-MS, allows the rapid measurement of major and trace element data for a wide range of elements that are below the detection limits of the electron microprobe (EMP). The quantification of LA-ICP-MS data of unknown samples is dependent on the analysis of calibration materials, such as NIST SRM 610 and 612. Currently, no published value is available for the concentration of Se in NIST SRM 612. We have used a combination of EMP, Sensitive High Resolution Ion Microprobe II (SHRIMP) and/or LA-ICP-MS techniques to measure the concentration of Selenium (Se) in NIST SRM 610, 612, 614 and a range of reference materials. The new reference value for Se in NIST 612 was then to measure the concentrations of Se in natural volcanic glasses.

Johnson, T. M., Bullen, T. D. (2004). Mass-Dependant Fractionation of Selenium and Chromium Isotopes in Low-Temperature Environments. In: Johnson, C. M., Beard, B. L., Albaréde, F. (Editors), Geochemistry of non-traditional stable isotopes. Reviews in Mineralogy and Geochemistry. Mineralogical Society of America, pp 289-317.

Palme, H, O'Neill, H. St.C. (2003). Cosmochemical Estimates of Mantle Composition, Treatise on Geochemistry. Elsevier Ltd., pp. 1-38.

XANES Analysis of Ni & Co in silicate glass: A Preliminary Investigation of Pressure Induced Changes in Their Coordination Environment

Jesse Jones[1], Hugh St.C. O'Neill[1] and Andrew Berry[2]

1 Research School of Earth Sciences, Australian National University, Canberra, ACT 0200, Australia
2 Department of Earth Science and Engineering Imperial College London, South Kensington London SW7 2AZ United Kingdom

The XANES region of the x-ray absorption spectrum (typically within 30-50 eV of the absorption edge) is strongly sensitive to both formal oxidation state and local coordination chemistry of the element under analysis. Pre-edge features in many transition-metal k-edge spectra provide a qualitative means to determine their coordination environment. Whilst s-p (orbital) is the primary transition for Ni and Co (1s core electron) K-edge spectra, elements of their pre-edge features reflect the degree to which local geometry around the absorbing atom allows hybridization of p-d orbitals, increasing the availability of transition states for the 1s core photo-electron and hence the pre-edge absorption intensity. The extent (if any) to which the intensity and shape of these pre-edge peaks are seen to vary with pressure, indicates a change in allowable hybridization associated with shifts between octahedral, distorted octahedral and tetrahedral symmetry.

To examine the possibility of pressure induced changes in the coordination chemistry of Ni and Co in silicate melt (taking silicate glass as the closest available analogue to a liquid melt structure) a series of high pressure experiments was conducted using a piston-cylinder apparatus (at 1500^{o}) to produce uniform high pressure glasses at 10, 20, 30 & 40 kb for each element. XANES analysis of the experimental glasses was carried out at the KEK PF synchrotron, Tsukuba, Japan. After the appropriate data reduction, our results indicate that whilst Co shows no apparent shift in its coordination environment over the applied pressure range, a systematic change in the coordination symmetry of Ni can be seen to occur toward the upper 40 kb limit of the study. This shift to a lower pre-edge peak intensity at higher pressures suggests a transition from tetrahedral coordination, where increased p-d hybridization occurs at lower pressures, toward a more centro-symmetric octahedral symmetry reflected by the lower intensity 40 kb peak. Further experiments are planned to examine this shift over an expanded pressure range.

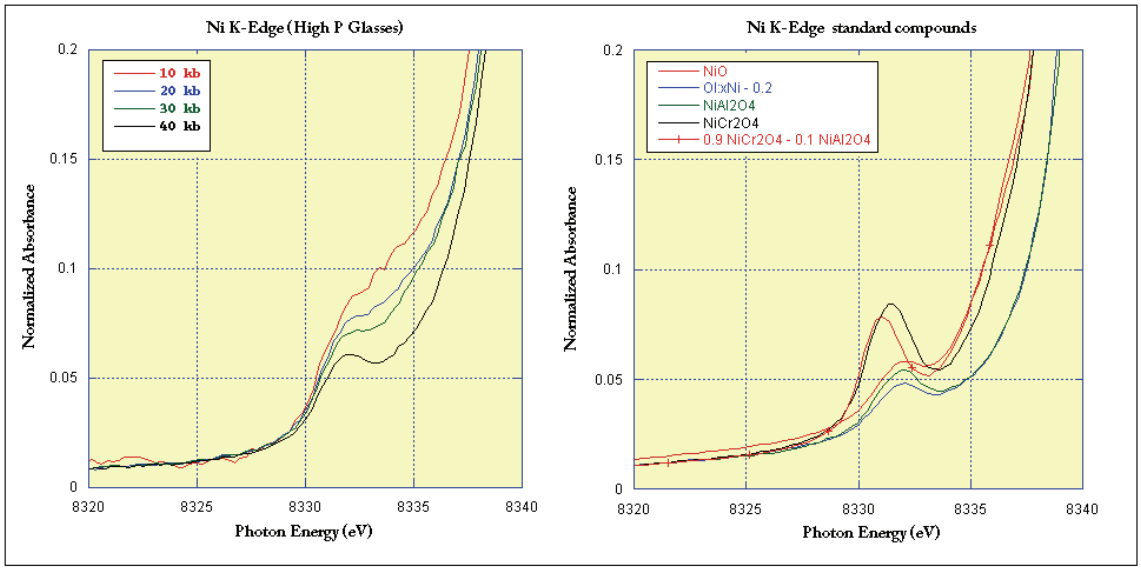
Ni K-Edge (High P Glasses)
10 kb
20 kb
30 kb
40 kb
Normalized Absorbance
Photon Energy (eV)
Ni K-Edge standard compounds
NiO
OlxNi - 0.2
NiAl2O4
NiCr2O4
0.9 NiCr2O4 - 0.1 NiAl2O4
Normalized Absorbance
Photon Energy (eV)

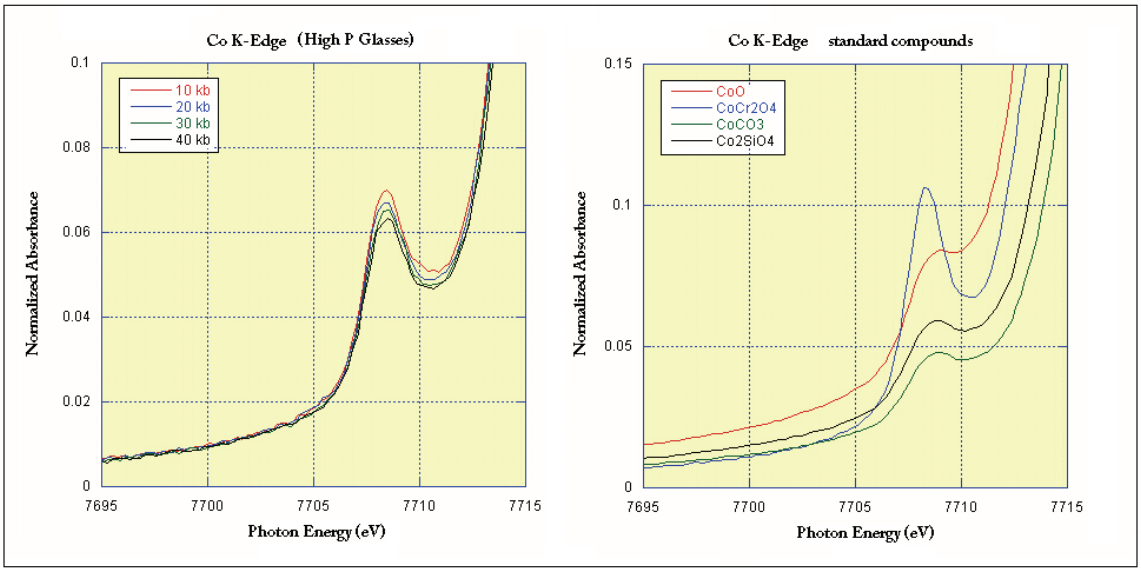
Co K-Edge (High P Glasses)
10 kb
20 kb
30 kb
40 kb
Normalized Absorbance
Photon Energy (eV)
Co K-Edge standard compounds
CoO
CoCr2O4
CoCO3
Co2SiO4
Normalized Absorbance
Photon Energy (eV)

Trial to establish muscovite-paragonite solvus by synthesis experiments

Huijuan Li [1], Hugh O'Neill[1], Jörg Hermann[1] and Ulli Troitzsch[1]

[1] *Research School of Earth Sciences, Australian National University, Canberra, ACT 0200, Australia*

Since the pioneering work of Eugster and Yoder (1955), numerous efforts have been made to study the nature of Ms-Pa solvus and its application as geothermometry by experimental work (Flux & Chatterjee, 1986 and references therein). Guidotti (1994) stated: "Unfortunately, field, experimental and thermodynamic investigations of Pg-Ms equilibria have yielded conflicting results".

In this study, we planned to obtain Ms-Pa solvus brackets at various T and 20 kbar by hydrothermal treatment of a variety of gel starting materials using Piston-Cylinder apparatus. Paragonite can be stable at a wider temperature interval at 20 kbar and high pressure will contribute to a faster and closer approach to the equilibrium.

The XRD spectra of all the runs accord with the spectra of 2M1 polytype mica. Through a calibration curve expressing cell volume *V* (Å) as a function of X_{ms}, we can obtain the compositions of predominant K-rich mica which are plotted in Fig 1. For run C3170 at 700°C, 20kbar, single phase mica was formed (blue circle in Fig 1), of which similar compositions were got from probe (X_{ms}=0.645) and XRD (X_{ms}=0.622). For runs at 650°C, 20kbar with 50%Ms+50%Pa as starting material, two phases of micas coexist, and the composition for K-rich mica is around X_{ms}=0.58. K-rich mica with X_{ms}=0.6587 was formed and Na-rich mica decomposed to Jadeite and Kyanite in run D1004 at 600°C, 20kbar. We obtain a graphical Ms limb of the solvus which locates at lower temperature than it should be according to the models in Chatterjee & Flux (1986) and Roux & Hovis (1996).

Eugster HP, Yoder HS (1995) Micas: The join muscovite-paragonite. *Carnegie Inst. Washington Yearbook* 54, 124-126

Guidotti CV, Sassi FP, Blencoe JG, Selverstone J (1994) The paragonite-muscovite solvus: I P-T-X limits derived from the Na-K compositions of natural, quasibinary paragonite-muscovite pairs. *Geochimica et Cosmochimica Acta* 58, 2269-2275

Chatterjee ND, Flux S (1986) Thermodynamic mixing properties of muscovite-paragonite solid solutions at high temperatures and pressures, and their geologic applications. *Journal of petrology* 27, 677-693

Roux J, Hovis GL (1996) Thermodynamic mixing models for muscovite-paragonite solutions based on solution calorimetric and phase equilibrium data. *Journal of petrology* 37, 1241-1254

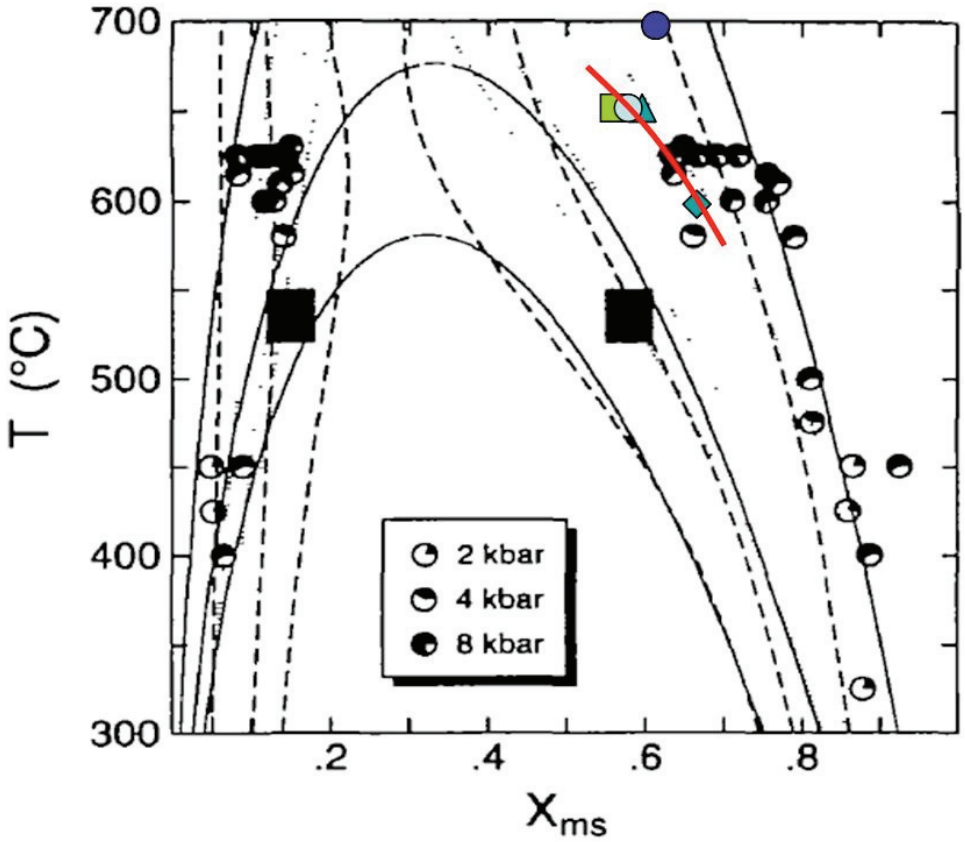

Figure 1. Comparison of results in this study with the solvi calculated at 2, 6 and 15 kbar using Model D (continuous lines), Model A (dashed lines) and chatterjee & Flux (1986) (dotted lines). The rectangular boxes and circles are compositions for natural micas from Grambling (1984) and Guidotti et al. (1994). (from Roux & Hovis, 1996)

The redox state of terrestrial basalts determined by V/Sc olivine-melt partitioning data

Guil Mallmann[1], Hugh O'Neill[1], Frances Jenner[1], Marc Norman[1], Steve Eggins[1], Richard Arculus[1] and Chris Ballhaus[2]

[1] Research School of Earth Sciences, Australian National University, Canberra, ACT 0200, Australia
[2] Mineralogisch-Petrologisches Institut, Universität Bonn, Poppelsdorfer Schloss, Bonn 53115, Germany

The dependence of the partitioning of V between olivine and silicate melt ($D_V^{ol/m}$) on oxygen fugacity was used to estimate directly the redox state of primitive terrestrial basaltic and picritic magmas at that stage in their evolution when they begin to crystallize olivine. The effect of other variables was accounted for by rationing $D_V^{ol/m}$ to $D_{Sc}^{ol/m}$, because the partitioning of Sc, a redox insensitive element having approximately the same incompatibility at terrestrial oxygen fugacities, is shown to depend rather similarly on melt composition. The method was calibrated on basaltic compositions equilibrated in the laboratory (one atmosphere) at QFM and QFM-2.7 between 1300 and 1400°C. We demonstrated that this method can be effective over the entire range of redox conditions observed in geological and cosmochemical materials, and therefore may serve as a universal redox indicator in olivine-phyric mafic volcanic rocks. Our preliminary assessment indicates accuracy in relative oxygen fugacity between 0.2 to 0.5 log units, but precision typically better than ±0.2 log units. The method was applied to 41 mid-ocean ridge (MORB), 25 ocean island (OIB), and 13 island arc (IAB) recent primitive basalts and picrites. The data indicate that MORBs and OIBs record a very restrict range of redox conditions, between QFM and QFM+1, with no clear distinction between them. However, IABs record consistently more oxidizing conditions, ranging from QFM+0.5 to QFM+3 (average at QFM+1.7). Except for MORBs, for which the data cluster exactly on the maximum redox condition ever reported, the results presented here are in good agreement with previous estimations using various methods in minerals and melts.

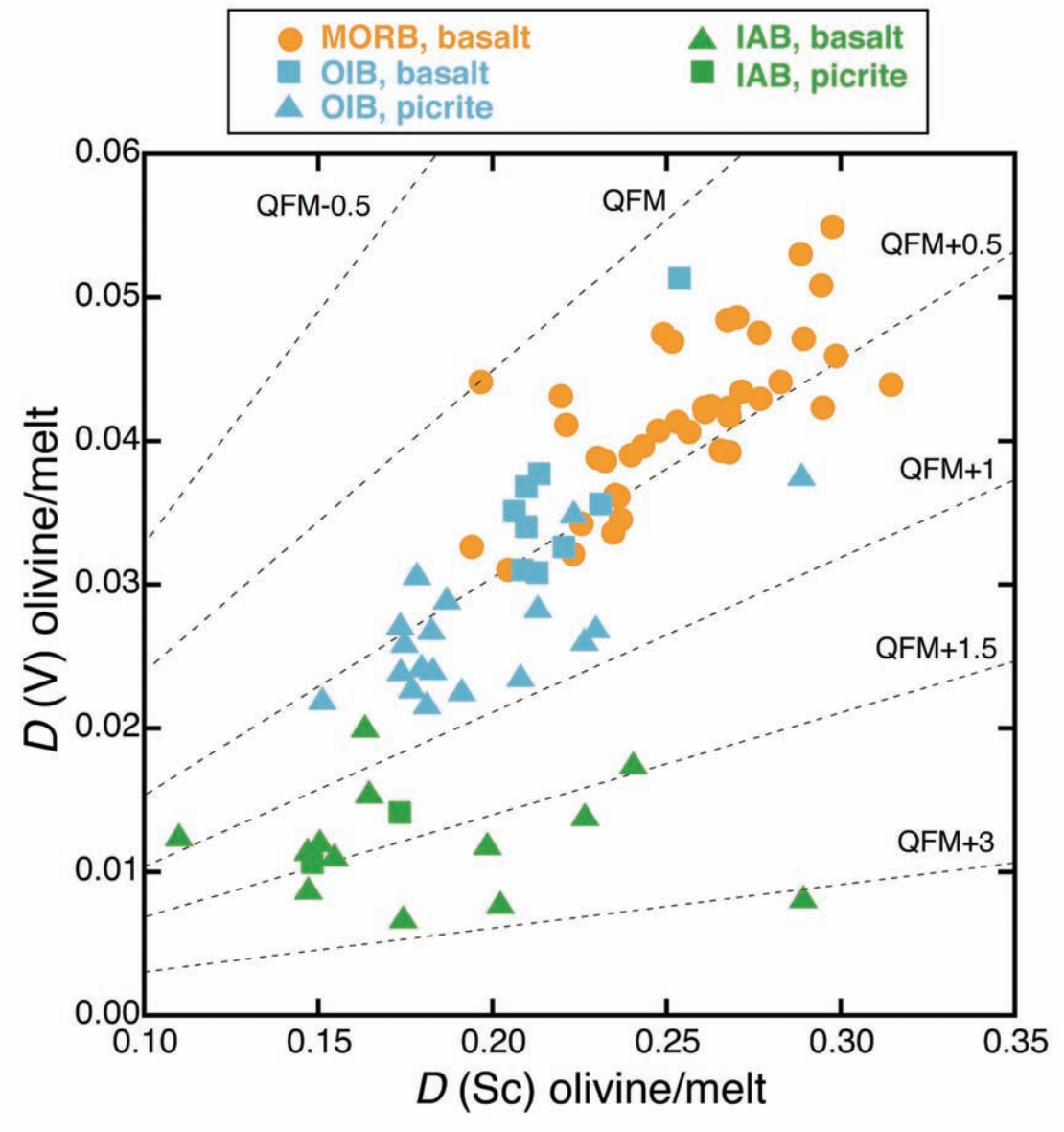

Figure 1. Partition coefficients obtained empirically for V and Sc between olivine phenocryst and silicate melt (glass or matrix). The positive correlation between is indicative of effects (possibly melt composition) other than oxygen fugacity. The dashed lines, illustrating values of oxygen fugacity relative to the QFM buffer, were calculated based on the experimental partitioning data.

Experimental investigation of fluid transfer in sub-arc mantle conditions

Cassian Pirard[1] and Jörg Hermann[1]

[1] *Research School of Earth Sciences, Australian National University, Canberra, ACT 0200, Australia*

Fluid transport from the subducted slab to the locus of partial melting in the mantle wedge in volcanic arcs is a process which is still strongly debated. Two end member mechanisms are considered: 1) porous fluid transfer through the mantle or 2) focused fluid flow in dykes/channels. These two processes are very different and the composition of reacted fluids arriving at the locus of partial melting in the mantle wedge must have different trace element signatures depending on which process is involved.

The main goal of this experimental study is to constrain the change in composition of the fluid as a result of these two ways of fluid transport. Experiments were performed on natural San Carlos olivine representing a simplified mantle and various pre-synthesized, trace element doped, hydrous felsic glass identified as slab-extracted melts (Fig.1)(Hermann & Spandler, 2008). Synthesis piston cylinder experiments were carried out in gold capsules for a week in the range 700°-1100°C and 35kbar which represent average values for the extraction of slab-fluids into the mantle (Fig.2).

Porous fluid transport was simulated by mixing a 1 to 4 ratio of fine grained hydrous felsic glass with fine grained olivine. One end of the capsule was filled with carbon spheres in order to collect the reacted quenched fluid at the end of the run. These mixed charges show an olivine-orthopyroxene-biotite±garnet± amphibole assemblage in equilibrium with a fluid (Fig. 1a). Fluid traps collected in K_2O-rich experiments (amphibole barren) were analyzed with laser ablation ICP-MS. Fluid composition was calculated using Ce as internal standard and normalized on the initial felsic glass. It appears that the crystallization of phlogopite has a strong impact on the composition of the fluid. The K_2O/H_2O ratio is considerably diminished (Fig. 2) and the LILE have a strong affinity to follow potassium in phlogopite whereas LREE, MREE and HFSE tend to be enriched into the fluids. In the case of the H_2O-rich experiments, the presence of amphibole and biotite modify the system. Fluids are less abundant and most of the initial starting material is retained in a hydrous peridotitic mix.

Focused fluid was simulated by a layered experiment of hydrous felsic glass overlying coarse olivine grains. A carbon spheres fluid trap was placed over the olivine layer. Significant differences are observed in this type of experiment compared to the mixed experiments. A reaction zone consisting of an orthopyroxenite layer ±garnet only occurs at the interface between olivine and the felsic glass and neither phlogopite nor amphibole has been observed (Fig.1b). In consequence, the glass composition is very similar to the starting composition and the shielding provided by the garnet-orthopyroxenite reduced strongly interactions with olivine, keeping the K_2O/H_2O high. LILE remain high in the quenched glass and REE and HFSE are less affected with respect to the initial starting glass.

These two types of experiments show that there are strong differences in transport behaviour of LILE in the mantle wedge dependent on the fluid flow mechanism. The high K_2O/H_2O and LILE contents observed in arc lavas suggest that fluid transfer in sub-arc conditions can occurs by channelled flow. In case of porous flow, fluids are strongly affected by the crystallization of biotite and LILE are retained in the residue (Fig. 2). However, the melting of such hydrous peridotite residues containing both micas and amphiboles could potentially lead to the formation of arc lavas as well.

Hermann J, Spandler C (2008) Sediment melts at sub-arc depths: an experimental study. *Journal of Petrology* **49**:717-740

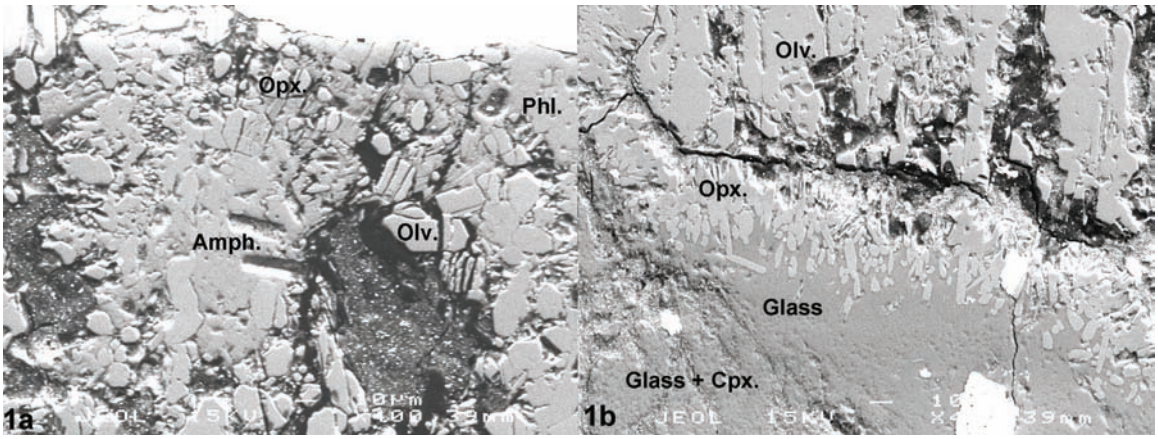

Fig.1. 1a. H_2O-rich mixed experiment showing anhydrous phases (Olivine, Orthopyroxene) and hydrous phases (Biotite, Amphibole) 1b. H_2O-rich layered experiment showing the contact zone between the olivine and the glass, forming an orthopyroxene layer.

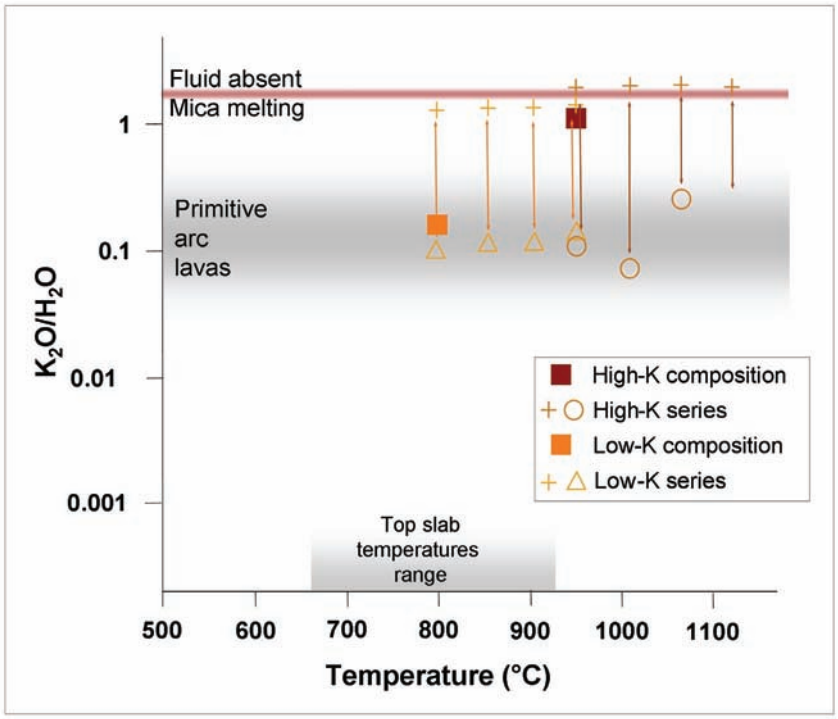

Fig.2. Composition of the different K-bearing phases of these sets of mixed experiments. Full squares are starting compositions; crosses are phlogopite K_2O/H_2O ratios; circles are quenched fluids and triangles give the amphibole composition.

Archean granitoid magmatism and the chemical evolution of the cratonic lithosphere

Robert Rapp[1], Herve Martin[2], Didier Laporte[2], and J-F. Moyen[3]

[1] *Research School of Earth Sciences, Australian National University, Canberra, ACT 0200, Australia*
[2]*Laboratoire Magmas et Volcans, Universite de Blaise Pascal, Clermont-Ferrand, France*
[3]*Department of Geology, University of Stellenbosch, Matteland, South Africa*

Although there is indirect evidence for the existence of continental crust on Earth more than 4.0 Ga ago (Harrison et al., 2005), no intact, preserved fragments of continents have been found. This begs the question when and how did the first truly "nondestructible" continents form? The development of deep (>200 km), old and chemically refractory roots to the continents in the underlying lithospheric mantle appears to be a critical stage in the physical and chemical evolution of Earth's cratons, the old and stable nuclei of the continents. Without roots in the underlying sub-cratonic lithospheric mantle, the preservation of large continental masses over billions of years may not have been possible. Ongoing experimental and field-based petrologic research over the past several years has led to an improved understanding of the genetic links between granitoid magmatism on the early Earth and the development of their roots in the cratonic lithosphere.

It is well established from studies of Archean (~2.5-4.0 Ga old) granite-greenstone and high-grade gneiss terranes around the world that the granitoid plutons comprising the "continental" component in these areas are dominated by rocks of the trondhjemite-tonalite-granodiorite (TTG) suite of granitoids. A number of experimental studies have previously shown that TTG "magmas" can be generated by low-moderate degrees of partial melting of hydrous "metabasaltic" crust in the garnet-amphibolite-eclogite facies (e.g., Rapp and Watson, 1995; Rapp et al., 2003), and thus tectonic processes that lead to overthickening or recycling (subduction?) of secondary basaltic (oceanic?) crust could also culminate in TTG-forming dehydration melting reactions. In the meantime, detailed field-based petrologic and geochemical studies in a number of granite-greenstone terranes (e.g., the Superior Province of Canada and the Pilbara of Australia; see Smithies and Champion, 2000) had identified another suite of Late Archean "post-kinematic" granitoid intrusives (the "sanukitoid" suite), that possessed "primitive" (i.e., mantle-like) characteristics overprinted onto an overall "TTG-like" geochemical signature, suggesting a hybrid lineage with a significant mantle contribution somewhere along the way.

In an effort to constrain the petrogenesis of sanukitoid magmas, we began a series of high-pressure laboratory experiments at 3-5 GPa in which TTG melts were allowed to react with (and assimilate) a peridotite mineral assemblage (Rapp et al., 1999). Our latest results show that primitive (high-magnesium) granitoids (andesites) comparable to Late Archean sanukitoids result from the equilibration of TTG melts with olivine-bearing mantle phase assemblages (Rapp et al., 2009). The resulting olivine-free garnet pyroxenite and garnet websterite reaction residues are currently being characterized in terms of their major- and trace-element compositions, for subsequent comparison with mantle xenoliths from the subcratonic mantle lithosphere.

Harrison, TM, Blichert-Toft, J, Muller, W, Albarede, F, Holden, P, Mojzsis, SJ (2005) Heterogeneous Hadean Hafnium: evidence of continental crust at 4.4 to 4.5 Ga. Science 310, 1947-1950.

Rapp, RP, Watson, EB (1995) Dehydration melting of metabasalt at 8-32 kbar: Implications for continental growth and crust-mantle recycling, *Journal of Petrology* **36**, 891-931.

Rapp, RP, Shimizu, N, Norman, MD, Applegate, GS (1999) Reaction between slab-derived melts and peridotite in the mantle wedge: experimental constraints at 3.8 GPa. *Chemical Geology* **160**, 335-356.

Rapp, RP, Shimizu, N, Norman, MD (2003) Growth of early continental crust by partial melting of eclogite. *Nature* **425**, 605-609.

Rapp, RP, Yaxley, GM, Norman, MD (2008) Genetic relations between Archean granitoid magmatsim and the chemical evolution of subcratonic lithospheric mantle: experimental constraints at 3-4 GPa. *Lithos* Special Volume: 9th International Kimberlite Conference (submitted).

Smithies, R.H. and Champion, D.C. (2000). The Archaean high–Mg diorite suite:

links to tonalite–trondhjemite–granodiorite magmatism and implications for Early Archaean crustal growth. *Journal of Petrology* **41**, 1653–1671.

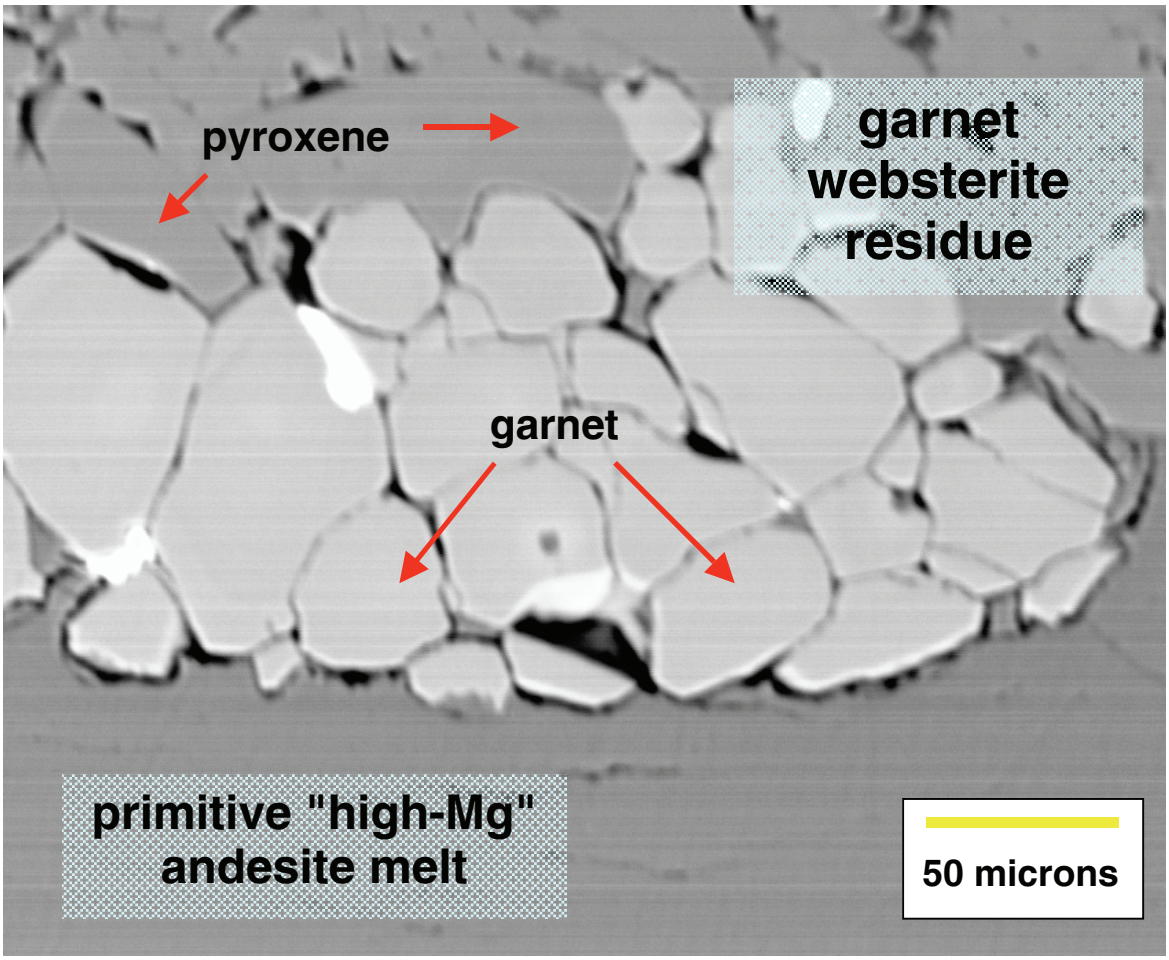

Synthesis and crystal structure of $CuZrTiO_5$: a new inorganic compound

Ulrike Troitzsch[1], Andrew G. Christy[1], David J. Ellis[1] and Anthony C. Willis[2]

[1] *Research School of Earth Sciences, Australian National University, Canberra, ACT 0200, Australia*
[2] *Research School of Chemistry, Australian National University, Canberra, ACT 0200, Australia*

A new inorganic compound, $CuZrTiO_5$, was discovered as a by-product of high-PT experiments with rutile [TiO_2] and baddeleyite [ZrO_2] that were fluxed with CuO. The compound was synthesized in pure form by sintering from the oxides at 1000°C under atmospheric pressure. It is bright green (Figure 1) and strongly pleochroic.

Its composition was confirmed with energy-dispersive x-ray analysis in the scanning electron microscope, and its crystal structure investigated with single-crystal and powder X-ray diffraction.

$CuZrTiO_5$ is orthorhombic, and crystallizes in space group $P2_12_12_1$, with unit cell dimensions a = 3.5871(3) Å, b = 6.6968(4) Å, c = 14.6679(9) Å, cell volume V = 352.35(4) Å, Z = 4, based on a single crystal refinement resulting in R = 0.032 and R_w = 0.079.

The crystal structure is topologically similar to that of In_2TiO_5 (*Pnma*) (Gaedwang et al.1993) but differs in space group and cation coordination (Figure 2). In $CuZrTiO_5$, the two types of In are replaced by Cu and Zr. While $CuZrTiO_5$ has relatively regular TiO_6 polyhedra (Ti-O = 1.84 - 2.18 Å), Zr is in 7+1 coordination (6 O at 2.10 - 2.27 Å and one at 2.811 Å) and Cu shows the 4+2 coordination characteristic of the Jahn-Teller effect. Four O surround Cu in an approximate square at 1.915 - 2.029 Å, while two more distant neighbours lie on opposite sides of the square at 2.565 and 2.591 Å.

In $CuZrTiO_5$, the cations are ordered into layers parallel to (001) of either pure Cu or alternating zigzag chains of Ti and Zr. This layered structure causes the distinct {001} cleavage of $CuZrTiO_5$ observed in the electron microscope (Figure 3).

Gaewdang T, Chaminade JP, Gravereau P, Garcia A, Fouassier C., Hagenmuller P, Mahiou R (1993) Crystal structure and luminescent properties of indium titanate. *Materials Research Bulletin* **28**:1051-1060.

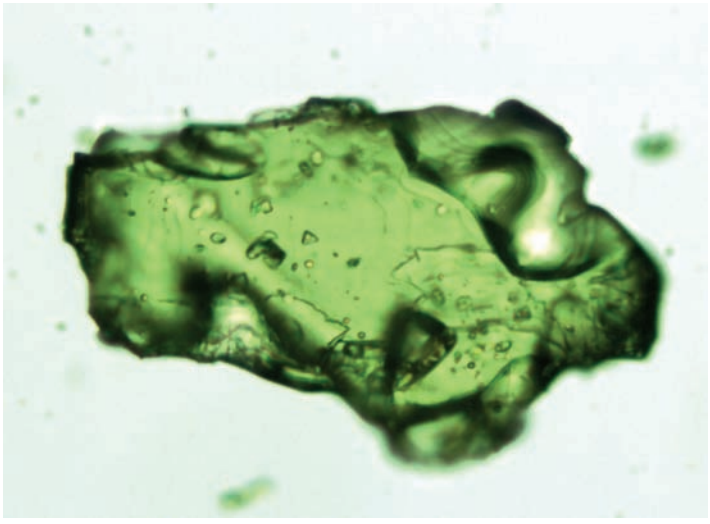

Figure 1.

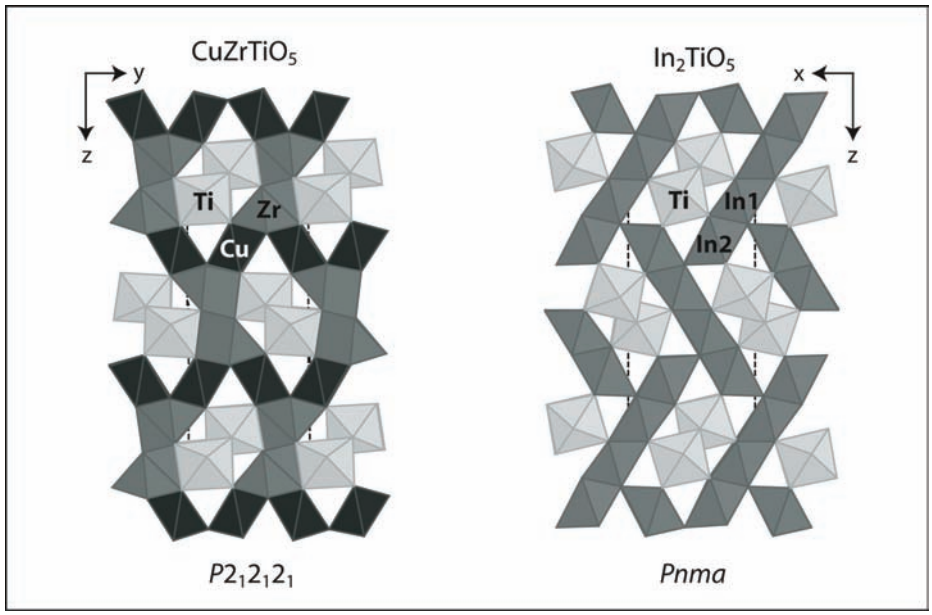

Figure 2.

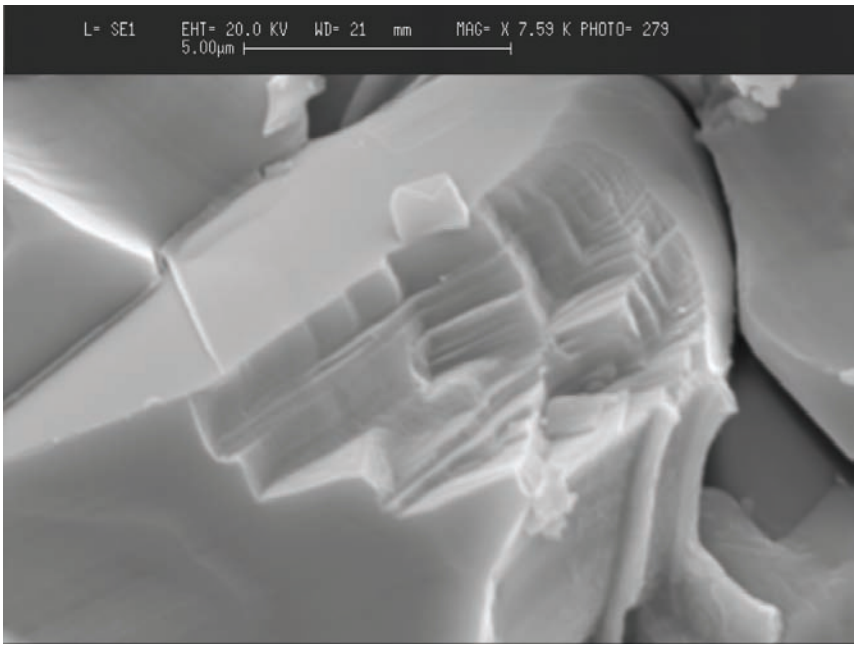

Figure 3.

Coupling between deformation processes and fluid flow in the Earth's crust

Stephen F. Cox

Research School of Earth Sciences, The Australian National University, Canberra, ACT, 0200

Experimental, field-based, microstructural and numerical modelling approaches are being used to explore several aspects of coupling between deformation processes, fluid transport and reaction, especially in fracture-controlled flow regimes.

In 2008, *field-based, modelling, microstructural and microchemical studies* are being used to further explore the growth of faults and fracture networks, and what factors lead to fluid flow becoming localised in certain parts of fracture controlled hydrothermal systems. The research has implications for understanding the localisation of hydrothermal ore deposits within fracture systems, and with minerals industry support, is providing new tools to help enhance exploration strategies. The work is also providing fundamental insights about the roles of reactive pore fluids in controlling fault mechanics and the growth of fracture networks.

Field and modelling studies, in the North Carlin gold systems in Nevada, have evaluated the role of co-seismic static stress changes in governing the distribution of aftershock activity in controlling localisation of fluid flow and related gold mineralisation within particular parts of fault networks.

A study of an Archaean, mesothermal gold system near Kambalda (WA), has shown how, during fault-valve behaviour near the base of the continental seismogenic regime, the relative rates of recovery of shear stress and pore fluid factors after slip events, impact on the internal structure of fault zones, as well as the nature and distribution of gold mineralisation.

In intrusion-related hydrothermal systems, the evolution of fluid pathways and the geometry, distribution, and other characteristics of vein systems, are governed by interactions between stress and fluid pressure states, and by the orientation of stress fields during and after magma emplacement. Stress states and the orientations of stress fields within active intrusive systems respond very dynamically to repeated cycles of inflation and deflation of fluid pressures due to migration of magma and hydrothermal fluids. Repeated variations in stress magnitudes and orientations can also be driven by sudden co-seismic stress relief and more gradual interseismic stress recovery associated with episodic, large earthquakes in convergent margin settings. Additionally, geodetic and seismological studies have demonstrated that episodic fluid migration, as well as cyclic changes in the orientations and magnitudes of stresses, occur on time-scales of years to decades in contemporary magmatic systems. This occurs especially in response to eruption cycles, emplacement of dyke swarms, and effects of nearby earthquakes. Indeed, stress change due to magma migration is likley to be a major driver of seismicity, and associated development of fracture-controlled fluid pathways, up to 15 km from the sites of magma movement. Small dynamic stress changes associated with remote, but large, earthquakes can also trigger microseismicity and attendant fracture propagation and fluid movement in magmatic systems.

A new project, as part of the ANU node of the Centre of Excellence in Ore Deposits, is using this modern understanding of the dynamics of magmatic systems as a basis for undertaking structural, microstructural and alteration studies to analyse the evolution of stress and fluid pressure states during the development of vein systems and faults in intrusion-related hydrothermal systems. The broad goal is to understand how the dynamic evolution of fracture-controlled fluid pathways impacts on the styles of flow

and ore deposition, as well as the distribution of mineralisation. In 2008, attention has focussed on the giant Porgera gold deposit (in the far western PNG highlands). Projects on other intrusion-related systems are being developed for subsequent years. A key early result is that fluid flow, in such fracture-controlled hydrothermal systems, is probably controlled by episodic breaching of substantially overpressured, magmatic fluid reservoirs at depth. Fluid pressure fluctuations are associated with repeated cycles of reservoir breaching and episodic, fluid-driven growth and sealing of fracture networks. These processes have important implications for ore deposition. In particular, large, transient hydraulic gradients promote rapid flow and potentially severe chemical disequilibrium in the ore fluid.

The mechanical and fluid pressure evolution of the Argo fault zone, St Ives goldfield, Western Australia: an example of an Archaean, shear-hosted, mesothermal gold system

Matthew A. Crawford[1] and Stephen F. Cox[1]

[1]*Research School of Earth Sciences, The Australian National University, Canberra, ACT, 0200*

The development of low displacement, moderate to high-angle reverse faults during the formation of the Argo gold deposit, within a tholeiitic gabbro host-rock, involved a four stage evolution of deformation and associated hydrothermal alteration. Fault zone evolution and Au mineralization were associated with high fluid flux, fault-valve behaviour in a severely-misoriented fault zone. The far-field maximum principal stress was approximately east-west and horizontal, and the far-field minimum principal stress was sub-vertical. The fault system developed at approximately 400°C in a transitional brittle-ductile regime, near the base of the continental seismogenic regime. Initial Stage 1 deformation involved ductile shear and the development of potassic (biotite-rich) alteration assemblages and associated reaction-weakening in shear zones; few quartz extension veins were formed. Stage 2 is marked by onset of predominantly brittle shear failure at elevated pore fluid factors, and was associated with widespread development of matrix-supported, dilational breccias in fault zones, and a change to sodic (albite-carbonate-quartz) alteration styles. Extension veins have limited development. Stage 3 is also dominated by brittle shear failure, and characterized by a change to quartz-carbonate assemblages in fault-fill veins and breccias. In contrast to Stage 2, large arrays of extension veins are well-developed adjacent to faults. In Stage 4, widespread sub-horizontal quartz-carbonate-biotite extension veins were developed, but shear failure was limited.

Failure mode diagrams in pore fluid factor ~ differential stress space (Figure 1) illustrate how the structural evolution and styles of mineralisation in the Argo fault system reflect a response to progressive changes in relative rates of change of pore fluid factor and differential stress during individual fault-valve cycles. High fluid fluxes and rapid rates of recovery of fluid pressures, relative to rates of recovery of shear stress after slip events, have maintained the system at near-lithostatic fluid pressures and very low differential stresses during gold mineralization.

The structural and rock mechanics study has been complemented by detailed microstructural, microchemical and stable isotope studies of hydrothermal alteration and vein mineral assemblages to characterise variations in the intensity and style of alteration in space and time in the Argo shear system. This work, together with analysis of gold grade distribution, is providing new insights about structural and geochemical controls on gold deposition at scales ranging from the deposit scale, down to metre-scales.

Laboratory studies of Dislocation Damping

Robert Farla[1], Harri Kokkonen[1], John Fitz Gerald[1], Auke Barnhoorn[1,2], Ulrich Faul[3] and Ian Jackson[1]

[1] Research School of Earth Sciences, Australian National University, Canberra, ACT 0200, Australia
[2] Now at Department of Earth Sciences, Utrecht University, 3508 TA Utrecht, The Netherlands.
[3] Department of Earth Sciences, Boston University, Boston, MA 02215, USA

Last year we presented some preliminary results on dislocation annealing in fine-grained synthetic olivine [1]. Since analyses of these results showed that dislocations can be preserved over laboratory timescales, the first experiments to search for dislocation damping in polycrystals have now been conducted.

Two similar deformed synthetic olivine specimens have been investigated so far. The first specimen, 6618, has been deformed in compression up to 2.3% strain, the second, 6646, to 22%. The resulting dislocation densities are 2.3 and 3.6 μm^{-2} respectively. The specimens were exposed to a maximum temperature of 1100°C, and to oscillating torques of 1 – 1000s periods at each temperature decrement, generating maximum shear strains of around 10^{-5}. The strains are sensed from displacements measured with parallel-plate capacitance transducers.

The first attenuation experiment in torsion on specimen 6616 yielded a surprise null result. This led to some calculations for resolved shear stresses in relation to deformation in compression or torsion and assuming that, at high temperatures, the dominant slip system for olivine involves slip in the [100] direction on the (010) glide plane. The main results are shown in figure 1 for [100](010) slip in a single crystal olivine. The two panels (a) and (b) represent deformation in compression and torsion respectively. The parameters α, and β (and γ) are the direction cosines relative to the crystal axes [α,β,γ] and some major crystal directions are labelled. In uniaxial compression, the resolved shear stress as indicated by the contours in (a) has its maximum value of 0.5 for compression parallel to $[110]_c$. The contours in panel (b) describe the azimuth-dependent resolved shear stress for different torsion axes. Note that torsional deformation around the $[110]_c$ is the least favoured orientation for stressing [100](010). In contrast, a cylinder axis parallel to $[111]_c$ (ie making equal angles with all 3 principal unit-cell axes) is a good trade-off if a single crystal were to be deformed in compression then transferred to attenuation measurements in torsion. For the case of polycrystalline olivine, preliminary calculations show that prior torsional deformation should increase the anelastic strain by 6-fold relative to prior compressional deformation.

Figure 2 shows measurements of Q^{-1} for both deformed specimens with different dislocation densities in comparison to a similar synthetic but undeformed olivine specimen. Only specimen 6646 with the higher dislocation density shows enhanced attenuation and only at the highest temperatures (> 1000°C). In nature, dislocation density should be in equilibrium with the prevailing tectonic stresses in the upper mantle. Dislocation damping will become progressively more important as the grain-boundary dissipation decreases with increasing grain size. Accordingly, dislocation damping could dominate in melt-free material under upper-mantle conditions.

Since the resolved shear stress calculations indicated the need, prior torsional deformation experiments will be done through a collaboration with the University of Minnesota in 2009. Also for single crystals we plan to investigate the possibility of deforming along $[111]_c$ in compression. For both materials, subsequent measurement of the forced torsional behaviour will proceed at ANU.

[1] Farla RJM, Kokkonen H, Fitz Gerald JD, Barnhoorn A, Faul UH and Jackson I (2008) Dislocation recovery in fine-grained synthetic olivine. In preparation for submission to *Physics and Chemistry of Minerals.*

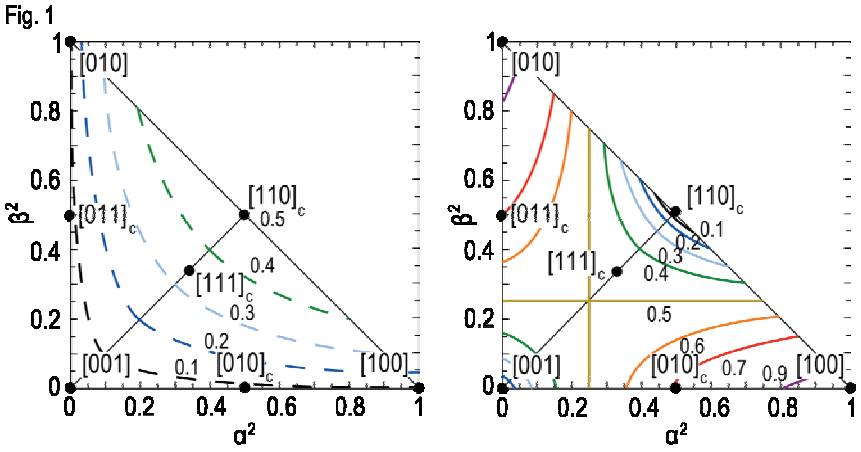

Figure 1. *Calculations showing the resolved shear stress (contours) for uniaxial compression (left) and torsion (right}*

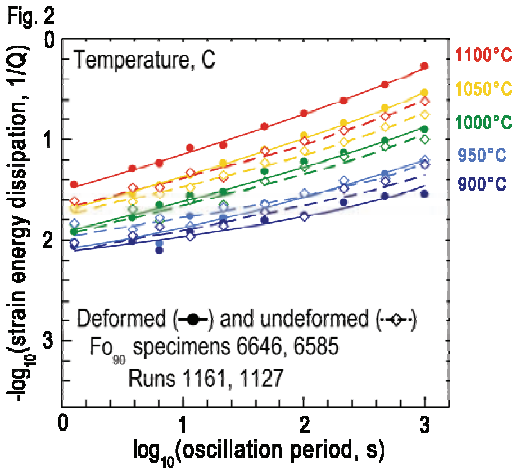

Figure 2: *Q^{-1} data for a deformed (6646) and undeformed specimen (6585).*

Development of fracture-controlled flow regimes and gold mineralisation, Porgera gold deposit, PNG

Angela Halfpenny[1] and Stephen F Cox[1]

[1]*Research School of Earth Sciences, The Australian National University, Canberra, ACT 0200*

Within the framework of the rapidly developing understanding of the dynamics of stress and fluid pressure regimes in contemporary, active magmatic systems, this project is exploring how stress states, stress field orientations and fluid pressures evolved during the development of the large, intrusion-related, hydrothermal gold system at Porgera in the highlands of Papua New Guinea. Fieldwork is being used to document the geometries and styles of vein systems, their overprinting relationships, and relationships to growth of fault networks. This is allowing us to examine how stress states, fluid pressure regimes, and the orientations of stresses evolved during the multi-stage evolution of the hydrothermal system. We are also evaluating what processes drove the growth of fracture-controlled flow networks and the evolution of fluid pathways. A key goal is to understand how the evolution of fracture-controlled fluid pathways and reactions impacts on the distribution of economic mineralisation in multi-stage, intrusion-related hydrothermal systems.

Work in 2008 has focussed on developing a 4D understanding of the evolution of vein distribution, geometries and internal textures during five distinct stages of vein development. The Porgera gold deposit exhibits at least two gold-bearing vein formation stages. The development of the richest vein-hosted Au mineralisation is associated with the growth of several low-displacement faults, which exhibit a complex kinematic evolution involving both dextral and normal slip histories during mineralisation.

The varied internal structures of Au-bearing veins and fault zones, such as textural and mineralogical zoning, in some cases provide evidence for multiple opening and sealing events (Figure 1). Flow in such fracture-controlled hydrothermal systems is unlikely to have been continuous. Instead, flow is interpreted to have occurred as numerous, episodic pulses associated with repeated cycles of breaching of the overpressured, magmatic fluid reservoir by failure events. Breaching events are followed by propagation of fracture arrays driven by migration of a fluid pressure pulse, then progressive sealing of fractures as flow rates decay. Ongoing work is focusing on defining the architecture of major, ore-producing fluid pathways.

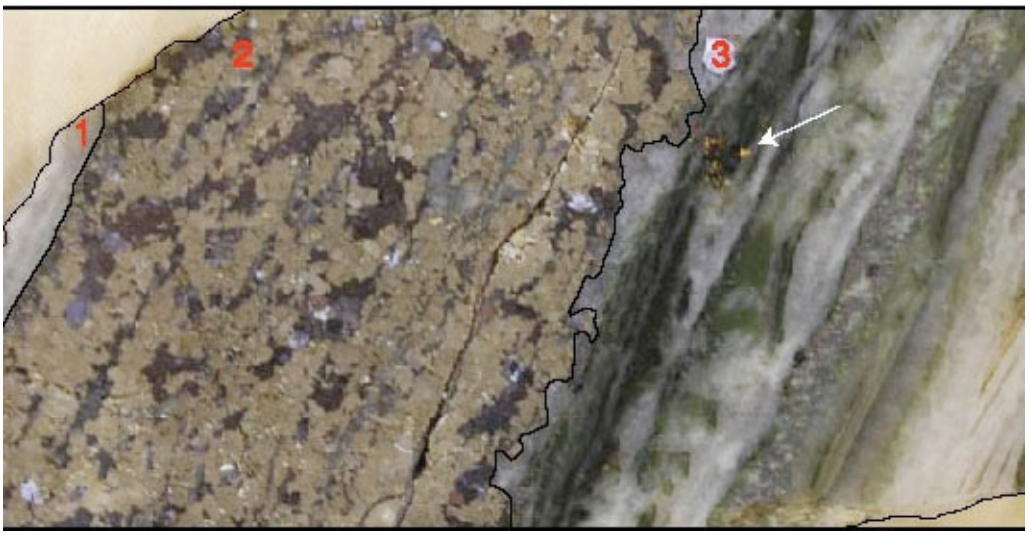

Figure 1. *a. The internal structure of a composite Stage 1 and Stage 2 vein. Section 1 and 3 represent the Stage 2 mineralisation, which exhibits crustiform quartz interlayered with roscoelite-rich layers. The gold is associated with the roscoelite-rich bands and a patch of gold is marked by the white arrow. Section 2 shows the Stage 1 vein.*

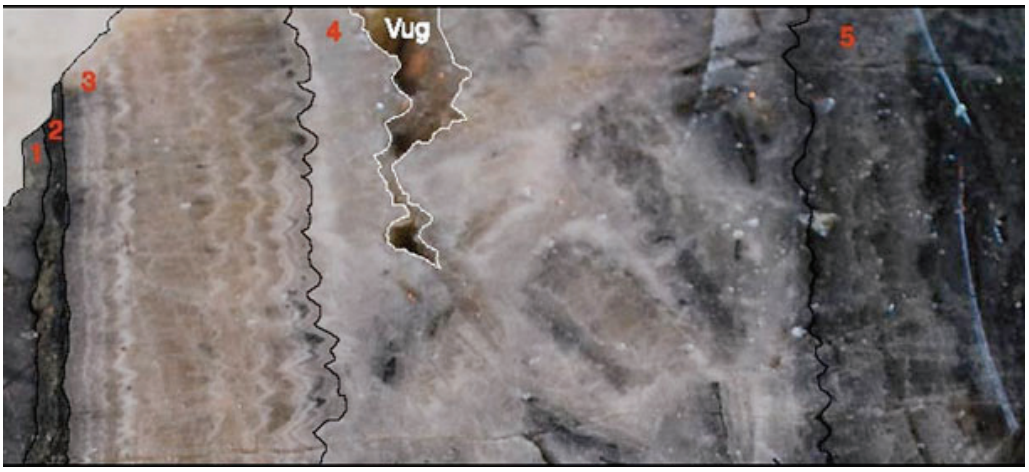

Figure 2. *Internal texture of a complex Stage 2 vein. Section 1 shows the wall rock. Section 2 is a pyrite-rich layer. Section 3 exhibits quartz-rich, crustiform banding which grades out into section 4 which shows a dilatational breccia containing wall-rock and quartz-rich clasts with a crustiform overgrowth. Section 4 also exhibits a vuggy centre to the vein. Section 5 exhibits crustiform banding and was in contact with the wall rock.*

Viscoelasticity, poroelasticity and seismic properties

Ian Jackson, John Fitz Gerald, Robert Farla, Harri Kokkonen, Hayden Miller

Research School of Earth Sciences, Australian National University, Canberra, ACT 0200, Australia

At sufficiently high temperatures in the Earth's interior, the mechanical behaviour changes from elastic to viscoelastic with profound implications for mantle rheology and also seismic wave speeds and attenuation. Such viscoelastic behaviour results from the stress-induced migration of vacancies and dislocations (extended defects reflecting prior or current deformation: see also Farla et al.). Equally, the stress-induced flow of fluids within cracked/porous media results in departures from elastic behaviour, termed poroelasticity. The following are highlights for 2008 of our ongoing study of rheology and seismic properties:

Hot-pressing and high-temperature deformation of titaniferous olivines (with U.H. Faul of Boston University): Work has continued this year towards an understanding of the influence of trace impurities on the rheology of fine-grained polycrystalline olivine. Specimens have been hot-pressed at 1300°C from sol-gel-derived Fo_{90} olivine precursors containing 0.1 wt % each CaO and TiO_2, and deformed at 1200-1300°C in compressive creep tests at progressively higher stress reaching ~300 MPa. Preliminary indications are that these materials (Fig. 1) undergo much more rapid grain growth than their Ti-free counterparts and are significantly weaker.

Seismic-wave dispersion and attenuation (with U.H. Faul, S.J.S. Morris of UC Berkeley, and D.R. Schmitt of the Univ. of Alberta): Our torsional forced-oscillation method for the study of high-temperature viscoelastic relaxation has recently been refined to take account of (i) compliance associated with frictional coupling between the specimen and neighbouring torsion rods, and (ii) significantly viscoelastic behaviour of the alumina control specimen [1]. Our published data concerning the shear modulus G and dissipation 1/Q for fine-grained melt-free and melt-bearing olivine have been re-processed with this improved strategy. Allowance for the compliant frictional coupling results in systematically higher G and lower 1/Q - especially for relatively coarse-grained (low-loss) materials tested at the highest temperatures (≥1200°C) and longest periods (>100 s). These effects are offset to some degree by allowance for the appreciably viscoelastic behaviour of the high-grade polycrystalline alumina control specimen. The interim result is an enhanced grain-size sensitivity of the viscoelastic relaxation (Fig. 2) meaning higher wavespeeds and lower attenuation on extrapolation to upper-mantle grain sizes. Additional experimental data for medium-coarse-grained materials are needed to underpin more robust extrapolation. Planned changes to the experimental procedure involving more active gripping of the cylindrical specimen and use of a single-crystal alumina control specimen may increase the signal/noise ratio for such low-loss materials. In a new initiative, our 'attenuation apparatus' is currently being modified to allow forced-oscillation measurements in extension/flexure, as well as torsion. Such measurements will allow the probing of poroelastic effects in cracked and fluid-saturated media that are analogues for upper-crustal rocks.

Modelling of elastic properties and equation of state (with B.L.N. Kennett): The thermodynamically consistent finite-strain model of Stixrude and Lithgow-Bertelloni (*GJI*, 2005) provides an attractive framework for the assessment and assimilation of experimental data concerning elastic properties and equation of state. The model requires the specification of 9 parameters: molar volume, (isotropic) bulk and shear moduli and their pressure derivatives, the effective Debye temperature, and the Grüneisen parameter and its volume and shear strain derivatives. We have explored the feasibility of using Sambridge's Neighbourhood Algorithm strategy (*GJI*, 1999) to undertake a guided search of the model space that is constrained simultaneously by

diverse experimental datasets as an alternative to iterative least-squares fitting. This approach has been tested on data for MgO including measurements of specific heat and thermal expansion, static and shock compression, and the pressure and temperature dependence of elastic wavespeeds. The search converged on a unique model that adequately represents most of the experimental data, but not before revealing tensions between marginally incompatible datasets.

[1] Jackson, I, A. Barnhoorn, Y. Aizawa and C. Saint. Improved experimental procedures for the study of high-temperature viscoelastic relaxation, *Phys. Earth Planet. Interiors* (in press).

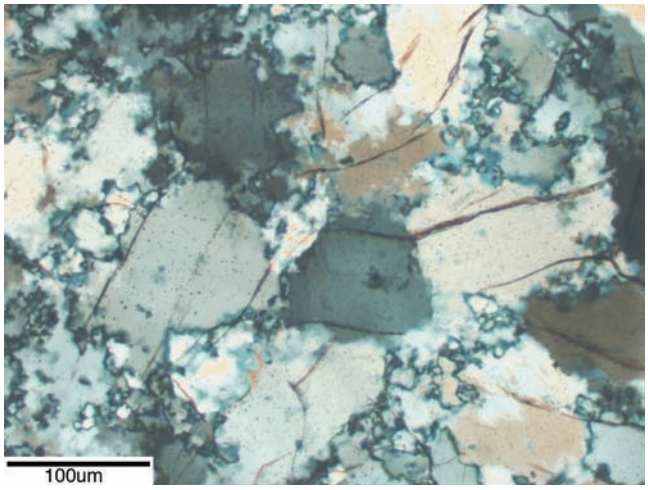

Figure 1

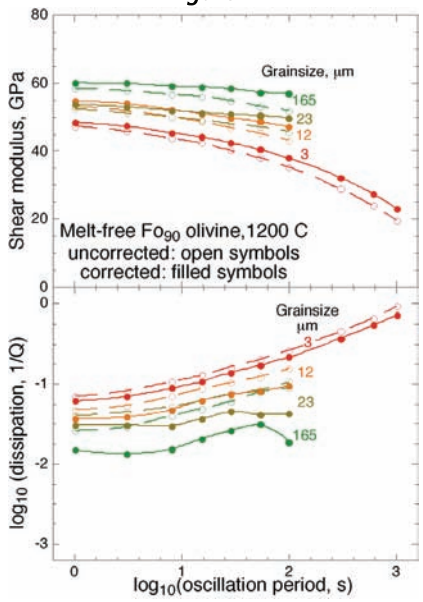

Figure 2

Exploration potential of stress transfer modelling in fault-related mineral deposits

Steven Micklethwaite[1,2], Stephen F. Cox[1]

[1] *Research School of Earth Sciences, Australian National University, Canberra, ACT 0200, Australia*
[2] *Now at: CODES, Private Bag 126, University of Tasmania, Hobart, TAS 7001, Australia*

This project applies the principles of the triggering mechanisms and triggering effects of active fault systems to understand gold mineralisation in ancient fault systems. Earthquakes generate small elastic stress changes, which in turn trigger other earthquakes and many thousands of aftershocks. Each aftershock is a fault slip event that enhances the permeability of the crust and high-frequencies of aftershocks tend to occur on faults with the same dimensions as those faults that host gold mineralisation in Australian gold camps. Previously, we have shown that at crustal depths of 10-20 km, orogenic-type gold deposits occur where co-seismic stress changes around a fault are likely to have triggered clusters of aftershocks (Micklethwaite and Cox, 2004, 2006; Micklethwaite, 2007). Therefore Stress Transfer Modelling helps us understand the dynamics of ancient fault systems and acts as a valuable predictive tool for the exploration industry.

Stress Transfer Modelling is now being extended to gold mineralised fault systems that developed in near-surface crustal environments (1-6 km) during episodes of normal faulting and high geothermal gradients, such as the Carlin-type gold deposits.

Both earthquakes and intrusive events generate small elastic stress changes in the crust, which have been linked to the triggering of thousands of aftershocks and the enhancement of permeability. We developed stress transfer modelling (STM) to understand the dynamics of ancient fault systems and act as a valuable predictive tool for the exploration industry (Micklethwaite and Cox, 2004, 2006; Micklethwaite, 2007). We have also been able to link co-seismic stress changes to wall rock damage generation and permeability, using Damage Mechanics Theory (Sheldon and Micklethwaite, 2007).

In 2008, we applied STM to near-surface hydrothermal environments (0.5-2 km; Carlin goldfield, Nevada), and deep hydrothermal environments (15-25 km; Agnew goldfield, West Australia). In the Carlin goldfield, mineralisation is broadly stratiform but also related to the upper tips of ~5 km-long normal dip-slip faults. Debate exists as to whether fluid migration was controlled by active fault processes, reaction-enhanced porosity generated in specific lithologies, or convection through fracture networks that were indefinitely open due to the low confining stresses of near-surface environments. In the Agnew goldfield, mineralisation forms a linear trend of pod-like bodies on the western limb of a regional fold. Fault rocks containing ore-grade mineralisation are dominated by ductile shear textures, with only small percentages of brittle deformation textures such as breccias and veins. Metamorphic grades suggest the goldfield formed in the mid-crust possibly at the base of a structure, but it was not clear whether visco-elastic creep processes, or co-seismic damage controlled fluid migration and mineralization.

In both case studies, STM predictions were made in three dimensions, and it was demonstrated that mineralization could be matched by the unique stress patterns generated at the tips of fault ruptures; indicating co-seismic elastic stress changes are a first-order control on permeability enhancement and mineralisation. This potentially represents a breakthrough for Carlin-related research and promises to resolve a long-standing debate.

Micklethwaite, S. and Cox, S.F., 2004. Fault segment rupture, aftershock-zone fluid flow, and mineralization. *Geology*, 32, 813-816.
Micklethwaite, S. and Cox, S.F., 2006. Progressive fault triggering and fluid flow in aftershock domains. *Earth and Planetary Science Letters*, 250, 318-330.
Micklethwaite, S., 2007. The significance of strings and clusters of fault-related mesothermal lode gold mineralization. *Economic Geology*. 102, issue 6, 1157-1164.
Sheldon, H.A. and Micklethwaite, S., 2007. Damage and permeability around faults: Implications for mineralization. *Geology,* 35, 903-906.

Mineralisation

Marie-Aude Bonnardot[1], Gordon Lister[1], Joe Kurtz[1] and Marnie Forster[1]

[1] *Research School of Earth Sciences, Australian National University, Canberra, ACT 0200, Australia*

Tectonic plate boundaries are the preferred location for economic mineralization, which appear to have been emplaced at specific time. This two-folded project proposes to re-examine tectonic evolution of the lithosphere along convergent and divergent boundaries. This project involves the development and application of the tectonic reconstruction tool, *Pplates*, in collaboration with Joe Kurtz and is also undertaken with the support from the DeBeers group.

Along convergent margins, subduction of lithospheric anomalies like seamount chain or oceanic plateau has the potential to vastly impact on the motion of tectonic plates. A famous example is the collision of the Ontong Java oceanic plateau along the New Guinea subduction zone to the north of Australia, which induced a drastic plate reorganisation involving subduction reversal in the SW Pacific. Based on previous works (Bonnardot et al., 2008), the first part of the project focuses on understanding the 3D geometry of slabs related to seafloor heterogeneities subduction and in particular, it focuses on the identification of slab tears, which may have a fundamental effect on the upper plate tectonic regime and on the porphyry deposits emplacement. We are currently revising the slab geometry in the Tonga, Sumatra and the South America subduction zones in regards to the tectonic evolution of the overriding plate, based on the analyse of the seismicity distribution and the stress regime within the involved lithospheric plates.

The second part of that project focuses on intracontinental rifting processes and aims at understanding the tectono-magmatic structures associated with anorogenic alkaline trends, for instance the relationship between transform faults/structural pattern of the mid-oceanic ridge and kimberlite emplacement.
Outcomes will allow refining plate motion in global tectonic reconstruction, as it will result in better quantifying the intraplate deformation that occurs during rifting initiation.

Bonnardot M.-A., Régnier M., Christova C., Ruellan E., Tric E. 2008. Seismological evidence for a slab detachment in the Tonga subduction zone. *Tectonophysics*, doi:10.1016/j.tecto.2008.10.01

Tectonic mode switches and the nature of orogenesis

Gordon Lister and Marnie Forster

Research School of Earth Sciences, Australian National University, Canberra, ACT 0200, Australia

The birth and death of many mountain belts occurs in lithosphere that over-rides major subduction zones. Roll-back creates a gravitational potential well into which the orogen collapses. This motion, coupled with stress guides, can "pull" an orogen apart. A slowing of roll-back (or of hinge retreat) means that the subduction flexure may subsequently begin to be "pushed back" or be "pushed over" by the advancing orogen. The consequence of such changes in relative motion is that orogenic belts are affected by abrupt tectonic mode switches. The change from "push" to "pull" leads to a sudden change from horizontal extension to horizontal shortening, potentially throughout the entire mass of the orogenic lithosphere that over_rides the subducting slab. The sequencing of these tectonic mode switches affects the thermal evolution of the orogen, and thus fundamentally determines the nature of orogenesis. In consequence high pressure metamorphic rocks are found in orogens characterized by push-pull sequences while high temperature metamorphic rocks are found in orogens characterized by pull-push sequences (Lister and Forster, 2008).

However the real complexity evident in the evolution of any orogen begins to emerge once we begin to consider movement in three dimensions. Motion orthogonal to an arcuate mountain front is typical of the geometry of collapse, where the orogen has spread over or been pushed over the adjacent foreland. For example it can reasonably be inferred that the Tibetan crust collapsed southward to create the modern arcuate shape of the southern boundary of the Himalayan mountain chain (see Figure below). In fact the mountain front defines an almost perfect small circle, with a radius of 1696 $\pm$ 55 km (Bendick and Bilham, 2001). GPS measurements suggest this flow is still occurring: present day movement is taking place in directions orthogonal to the modern arc (Jade et al., 2004). England and Molnar (2005) provide a convincing argument that crustal flow in Tibet is driven by the gravitational potential energy of the collapsing orogen: in their words, the orogen behaves more like a 'fluid' than a 'plate'. Forward motion of the Indian indentor is accommodated in the west by the left-lateral Chaman fault zone on the boundary between Afghanistan and Pakistan, and in the east (in Myanmar) by the right-lateral Sagaing fault zone.

The main focus of the India-Asia collision is now in the NW, under the ranges of the Hindu Kush. The impact of an indentor can be inferred from the paired clusters of strike-slip faults. In the South, the small-circle geometry of the Himalayan mountain front is diagnostic of the fluid-like behaviour of this collapsing orogen, reflecting the impact of radiating viscous flow driven by the gravitational potential energy of the collapsing Tibetan Plateau. Thrusts radiate orthogonally from the orogenic welt defined by the Tibetan plateau, southward, northward, and eastward. The effects of eastward flow of the collapsing Tibetan Plateau is particularly evident in the fold and thrust belt in Sichuan Province, the locus of several catastrophic earthquakes (yellow dots in Figure).

In contrast, in the Myanmar crust, there are two almost orthogonal competing movement patterns. Shortening occurs in the foreland fold and thrust belt because this zone accommodates WSW directed motion of crust flowing out from the Myanmar hinterland. The Sagaing wrench fault zone marks the locus of accumulating right-lateral offsets, periodically accommodating distortions caused by relative plate motion. At the same time concentric left-lateral strike-slip faults accommodate flow around the eastern syntaxis, causing distortion of the Sagaing Fault. These concentric

left-lateral strike-slip faults are most evident in the green lines that show the trend of fault plane slip vectors associated with left-lateral strike-slip earthquakes. As we move from north to south in a semicircle around the eastern syntaxis the movement direction associated with these earthquakes changes from towards ~90° to towards ~250°. This is a movement pattern that suggests mass flow in the deeper crust driven by the WSW-directed roll-back of the tearing Myanmar slab that lies beneath this zone.

Bendick, R., Bilham, R., 2001. How perfect is the Himalayan arc? Geology 29, 791-794, doi:10.1130/0091-7613(2001)029<0791:HPITHA>2.0.CO;2

England, P., Molnar, P., 2005. Late Quaternary to decadal velocity fields in Asia. Journal of Geophysical Research _110, B12401, doi:10.1029/2004jb003541.

Jade, S., Bhatt, B.C., Yang, Z., Bendick, R., Gaur, V.K., Molnar, P., Anand, M.B., Kumar, D., 2004. GPS measurements from the Ladakh Himalaya, India: preliminary tests of plate-like or continuous deformation in Tibet. Geol. Soc. Amer., Bull. 116, 1385–1391, doi:10.1130/B25357.1

Lister, G. and Forster, M. 2008. Tectonics mode switches and the nature of orogenesis. Lithos, in press.

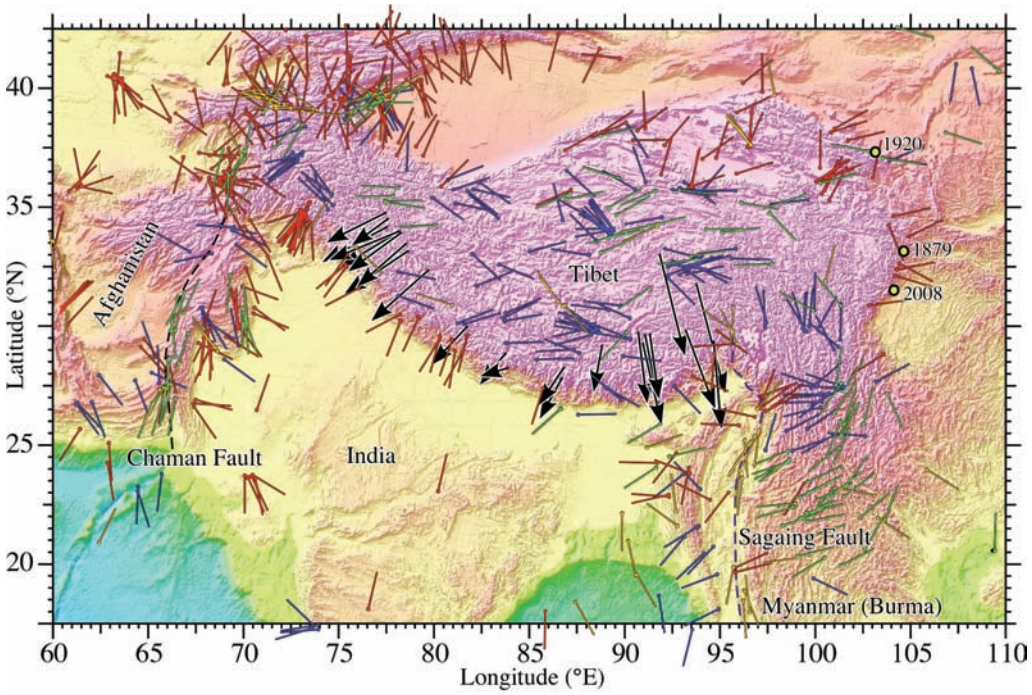

Figure 1. Geometry of a mountain front reflecting the impact of collapse driven by the gravitational potential energy of the orogen. Arrows show GPS motions relative to India (after Jade et al., 2004). The coloured slip lines stem from epicenters of 575 earthquakes in the period 1976-2006 in the depth range 0-60 km, as recorded in the Harvard Centroid Moment Tensor database (http:/ www.seismology.harvard.edu/CMTsearch.html). Map produced using Program eQuakes superimposed on images derived from NOAA (http://ibis.grdl.noaa.gov/cgi-bin/bathy bathD.pl). Each slip line shown represents a choice of one of two conjugate fault plane solutions derived from the centroid moment tensor: each choice based on details of the local geology. Thrusts (red), normal faults (blue), left-lateral strike-slip faults (green) and right lateral (yellow). Motion orthogonal to the mountain front is typical of the geometry of collapse where the orogen has spread over, or been pushed over the adjacent descending slab. Left-lateral Chaman fault zone (dashed) in the west (a). Right-lateral Sagaing fault zone (dashed) in the east (b).

Episodic emplacement of the Ladakh and Karakoram Batholiths

Lloyd White[1], Gordon Lister[1], Marnie Forster[1], Talat Ahmad[2] and Trevor Ireland[1]

[1] *Research School of Earth Sciences, Australian National University, Canberra, ACT 0200, Australia*
[2] *Department of Geology, University of Delhi, India*

Preliminary U-Pb SHRIMP dating of zircon grains from the Ladakh and Karakoram batholiths confirms some of the previously published ages for the two batholiths, but also indicates that older crust (possibly associated with the Tibetan slab) may have been involved with the Karakoram Bathoiith.

Samples of the Ladakh Batholith were collected from Khardung La and Chang La in Ladakh, NW India. These samples obtained an age of circa 58 Ma, similar to the age data published by earlier workers (e.g. Singh et al. 2007). This confirms that there was a strong phase of magmatism in the Ladakh Batholith at approximately 58 Ma.

Samples of the Karakoram Batholith were collected near Tangste Gompa and obtained an age of circa 32 Ma. One zircon grain from this sample also gave a late Permian age, which could indicate that older crust is associated with the Karakoram Batholith. One sample of a cross-cutting dyke collected in the Tangste Gorge (Figure 1 and 2) gave an age of circa 18 Ma. This is consistent with earlier published data that was associated with movement on the Karakoram Fault. Another sample of the Karakoram Batholith obtained an age of circa 102 Ma. Again, this is consistent with a date published for the same Batholith in Pakistan.

This study confirms many of the earlier published dates of the Ladakh and Karakoram batholiths. However, our preliminary work also shows that attention must be paid to younger phases of magmatism that cross-cut older phases of magmatism.

Singh, S. Kumar, R., Barley, M. E., Jain, A. K. 2007. SHRIMP U-Pb ages and depth of emplacement of Ladakh Batholith, Eastern Ladakh, India. *Journal of Asian Earth Sciences* **30**: 490-503

Figure 1. Aplite dyke cross-cutting an earlier migmatitic phase of the Karakoram Batholith, Tangste Gorge, Northwest India.

Figure 2. Tangste Gorge, Ladakh, Northwest India